Fluoride ion dynamics and relaxation in KSn_2F_5 studied by ^{19}F nuclear magnetic resonance and impedance spectroscopy

2003 J. Phys.: Condens. Matter 15 5341

(http://iopscience.iop.org/0953-8984/15/31/301)

INSTITUTE OF PHYSICS PUBLISHING JOURNAL OF PHYSICS: CONDENSED MATTER

J. Phys.: Condens. Matter **15** (2003) 5341–5352 PII: S0953-8984(03)57473-2

Fluoride ion dynamics and relaxation in KSn_2F_5 studied by ^{19}F nuclear magnetic resonance and impedance spectroscopy

M M Ahmad[1,3,4], M A Hefni[2], A H Moharram[2], G M Shurit[3], K Yamada[1] and T Okuda[1]

[1] Department of Chemistry, Graduate School of Science, Hiroshima University, Higashi-Hiroshima 739-8526, Japan
[2] Department of Physics, Faculty of Science, Assiut University, Assiut 71516, Egypt
[3] Department of Physics, Faculty of Education, Assiut University in The New Valley, El-Kharga, Egypt

E-mail: mmahmad@sci.hiroshima-u.ac.jp

Received 12 December 2002, in final form 26 May 2003
Published 23 July 2003
Online at stacks.iop.org/JPhysCM/15/5341

Abstract

Ion dynamics in the two-dimensional fluoride ion conductor KSn_2F_5 have been studied by ^{19}F nuclear magnetic resonance (NMR) and impedance spectroscopy. The electrical relaxation behaviour of the investigated material is represented in the conductivity and electric modulus formalisms. The values of the dc conductivity and the hopping frequency of mobile ions and their respective activation energies are estimated from the analysis of the conductivity spectra using Almond–West formalism. The activation energies for conduction and ion hopping processes are almost identical, with values of 0.53 and 0.54 eV, respectively, suggesting that the concentration of charge carriers is independent of temperature. The Roling scaling approach to the conductivity spectra is applied in order to gain insight into the temperature dependence of the relaxation mechanism. The scaling law successfully collapses the conductivity spectra into a single curve, indicating a temperature-independent relaxation mechanism. Moreover, chemical exchange simulation of the ^{19}F NMR spectra is introduced. The discrepancy between the values of the activation energies deduced from the electrical and NMR experiments are discussed according to Ngai's coupling model.

1. Introduction

Superionic conductors are those materials that allow the macroscopic movement of ions through their structure, leading to exceptionally high values of ionic conductivity whilst in the solid

[4] Author to whom any correspondence should be addressed.

state. They are not merely scientific curiosities, since they have a number of technological applications in a variety of electrical devices including batteries, sensors and electrochromatic displays. KSn_2F_5 belongs to the MSn_2F_5 family (M = Na, K, Rb, Cs, Tl and NH_4), which exhibits fluorine ionic conductivity [1–3]. The crystal structure of KSn_2F_5 at room temperature is trigonal with space group $P\bar{3}$ and $Z = 3$, where Z is the number of formula units per unit volume. Its trigonal structure contains infinite layers of $Sn_2F_5^-$ anions parallel to the *ab* plane and several fluoride ion positions are not perfectly occupied [1]. According to its structure, KSn_2F_5 can be considered as a two-dimensional fluoride ion conductor. The crystal exhibits a first-order structural phase transition to the superionic state at 428 K.

Electrical relaxation measurements are commonly used to characterize the dynamics of mobile ions in ionically conducting materials, including single crystals and polycrystalline and amorphous materials. Most of the measurements are performed in the frequency domain, and experiments are often performed and analysed in terms of the complex conductivity [4]

$$\sigma^*(f) = \sigma'(f) + \mathrm{i}\sigma''(f), \tag{1}$$

where $\sigma'(f)$ and $\sigma''(f)$ are the real and imaginary parts of the complex conductivity, respectively. Alternative representations of the same experimental data are the complex permittivity $\varepsilon^*(f) = \sigma^*(f)/\mathrm{i}\omega\varepsilon_0$, where ε_0 is the permittivity of the free space, and the complex electric modulus $M^*(f) = 1/\varepsilon^*(f)$. Although the same experimental data are used, different results and conclusions are derived from the different approaches, especially for the interpretation of the dependence of the electrical relaxation dispersion on the charge carrier concentration.

The real part of the complex conductivity of many ion-conducting materials exhibits a frequency dependence that is well approximated by the Almond–West expression of the form [5–7]

$$\sigma'(f) = \sigma_{\mathrm{dc}}[1 + (f/f_{\mathrm{H}})^n], \tag{2}$$

where σ_{dc} is the dc conductivity, f_{H} is the hopping frequency representing the crossover frequency from the dc to the dispersive conductivity region and the power law exponent n represents the electrical relaxation behaviour of the material, typically between 0.5 and 0.9 [8]. The frequency-independent conductivity σ_{dc}, found at low frequencies, represents the random process in which the ions diffuse via activated hopping throughout the lattice network. The dc conductivity could be given by the Nernst–Einstein relation as

$$\sigma_{\mathrm{dc}} = n_{\mathrm{c}} e \mu = \frac{n_{\mathrm{c}} e^2 \gamma \lambda^2}{kT} f_{\mathrm{H}}, \tag{3}$$

where n_{c} is the mobile charge carrier concentration, μ is their mobility, e is the electronic charge, γ is a geometrical factor for ion hopping ($\gamma = 1/6$ for isotropic materials), λ is the hopping distance and k is Boltzmann's constant.

However, the power-law dispersion indicates a non-random motion, wherein the ion motion is correlated. The range of the exponent n ($0.5 \leqslant n \leqslant 0.9$) indicates that this correlated motion is sub-diffusive due to a rapid back and forth displacement of the hopping ions. Several models have been proposed in order to determine the mechanism responsible for the electrical relaxation behaviour in crystalline and glassy materials [9–15]. Ngai *et al* [12, 13] have suggested that this correlated motion arises from some form of interionic interactions (ion coupling), leading to systematic change of the observed power-law exponent with ion concentration.

In contrast, Sidebottom [16] showed that the exponent n is independent of both temperature and ion concentration; instead, it is found to be influenced by the dimensionality of the ion's conduction space. In his recent survey of the power-law exponent obtained from ac conductivity

of ion conductors, the value of $n = 0.67$ was commonly observed for isotropic oxide glasses, while values of $n = 0.58 \pm 0.05$ and 0.3 ± 0.1 were observed for two-dimensional (Na β-alumina) and one-dimensional (hollandite) crystalline conductors, respectively, i.e. the exponent n decreases with decreasing dimensionality.

In the present work, we report measurements of electrical relaxation in KSn_2F_5 material represented by the conductivity and the electric modulus formalisms. The conductivity spectra were analysed in accordance with Almond–West formalism and the dc conductivity and the hopping frequency and their respective activation energies were determined. Moreover, comparison between the activation energies from electrical and nuclear magnetic resonance (NMR) measurements is introduced in accord with Ngai's coupling model.

2. Experiment

KSn_2F_5 was prepared from aqueous solution following Vilminot and Schulz [1]. Well developed crystals could be obtained under the hydrothermal condition at 440 K for several days. The thin plate precipitate of KSn_2F_5 was then filtered off immediately, washed with water and dried *in vacuo*. The product was characterized by x-ray powder diffraction and differential scanning calorimetry (DSC) measurements. Heat-flow type DSC measurements were performed using a sealed glass tube in the temperature range from 300 to 500 K at a heating rate of 4 K min^{-1}. DSC measurements showed one endothermic peak at 428 K, corresponding to the structural phase transition to the superionic state. X-ray diffraction data confirm that the crystal structure of KSn_2F_5 is trigonal with space group $P\bar{3}$ and $Z = 3$ at room temperature. Detailed structural analysis of the low- and high-temperature phases of KSn_2F_5 can be found elsewhere [17].

Impedance measurements were performed using a compressed powder pellet with carbon paints on both sides. The sample was then held between two spring-loaded electrodes. The impedance $|Z^*|$ and phase angle θ were measured with a computer interfaced HIOKI 3532 LCR meter (42 Hz–5 MHz) in the temperature range from 200 to 350 K with a heating rate of 1 K min^{-1}. ^{19}F NMR spectra were observed by means of a home-made pulsed spectrometer at 6.4 T. The single pulse sequence was applied and 64 free-induction decays (FIDs) were accumulated at each respective temperature. The dead time and the irradiation pulse length were 4.5 and 1 μs, respectively. The spectrum simulation program was developed by us using a software package, Mathcad[5].

3. Results and discussion

The frequency dependence of the real part of the conductivity, $\sigma'(f)$, for KSn_2F_5 is shown in figure 1 at several temperatures. The conductivity spectra in figure 1 exhibit common features usually found in ionic conductors. At low frequencies, random diffusion of the ionic charge carriers via activated hopping gives rise to the frequency-independent dc conductivity. However, with the increase in frequency, $\sigma'(f)$ shows a dispersion, which shifts to higher frequencies with increasing temperature. At high temperatures, $\sigma'(f)$ is found to decrease with decreasing frequency in the low-frequency region due to space charge polarization at the blocking electrode.

We have analysed the conductivity spectra in figure 1 using Almond–West formalism, equation (2), in order to determine the values of the dc conductivity, σ_{dc}, and the hopping frequency, f_H, of the mobile ions. However, it is observed in figure 1 that the conductivity data are highly affected by electrode polarization, especially at high temperatures. Accordingly, it is

[5] MathSoft International, Knightway House, Park Street, Bagshot, Surrey GU19 5AQ, UK.

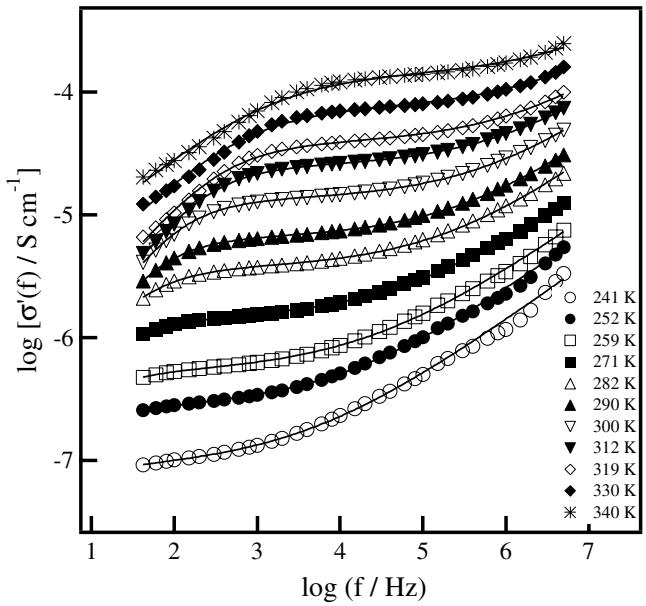

Figure 1. Conductivity spectra for KSn_2F_5 at several temperatures. The solid curves are the best fits by equation (6).

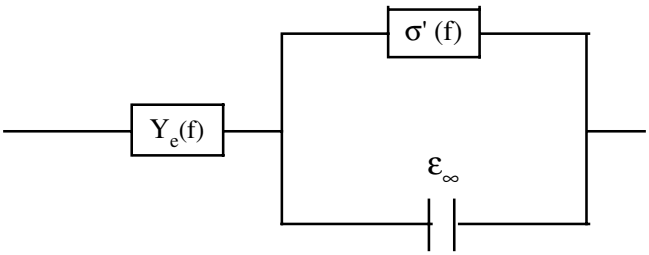

Figure 2. Equivalent electric circuit used for simulation of the conductivity spectra of KSn_2F_5. The quantities Y_e, $\sigma'(f)$ and ε_∞ are defined in equation (6).

necessary to include the electrode polarization effect in the fitting procedure of the conductivity spectra in order to obtain reliable values of the dc conductivity and the hopping frequency. The electrode impedance can be modelled in terms of a constant phase element (CPE) in series, as shown in figure 2, with the bulk conductivity of the sample [18]. The admittance of the CPE and the bulk complex conductivity are expressed as

$$Y^*_{\mathrm{CPE}} = Y_{\mathrm{e}} f^a [\cos(a) + \mathrm{i}\sin(a)], \tag{4}$$

and

$$\sigma^*(f) = \sigma'(f) + \mathrm{i}2\pi f \varepsilon_0 \varepsilon_\infty, \tag{5}$$

where Y_e and a are parameters for the electrode admittance, ε_∞ is the dielectric permittivity at the high-frequency limit and $\sigma'(f)$ is the real part of the bulk ac conductivity defined by equation (2). Then, the real part of the total complex conductivity for the bulk and the electrode is given by [18]

$$\sigma'_{\mathrm{T}}(f) = \frac{Y_{\mathrm{e}} f^a [\sigma'(f) Y_{\mathrm{e}} f^a + \sigma'^2(f)\cos(a) + (2\pi f \varepsilon_0 \varepsilon_\infty)^2 \cos(a)]}{\sigma'^2(f) + 2Y_{\mathrm{e}} f^a [\sigma'(f)\cos(a) + 2\pi f \varepsilon_0 \varepsilon_\infty \sin(a)] + (Y_{\mathrm{e}} f^a)^2 + (2\pi f \varepsilon_0 \varepsilon_\infty)^2}. \tag{6}$$

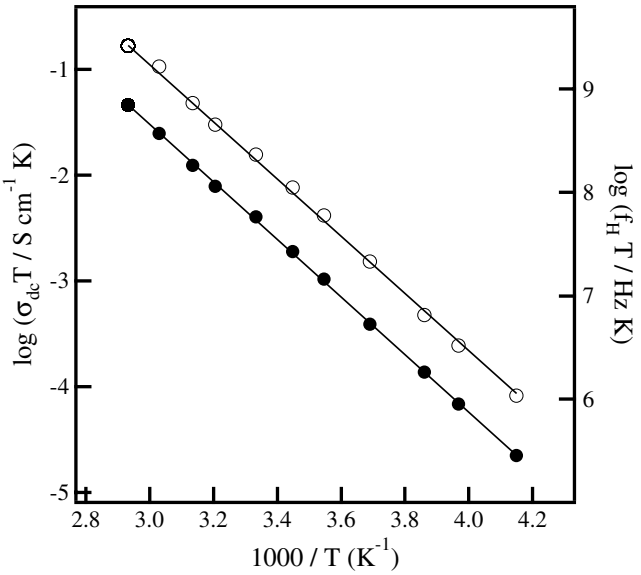

Figure 3. Temperature dependence of the fitting parameters, the dc conductivity σ_{dc} (solid circle) and the hopping frequency f_H (open circle); the solid lines are the straight-line fits of the data.

We have fitted the conductivity spectra of KSn_2F_5 by equation (6) using Y_e, a, σ_{dc}, f_H and n as variable parameters. Such fits at different temperatures are shown in figure 1. It is observed that equation (6) can fully describe the conductivity spectra, including the electrode polarization region at low frequencies. The value of the power-law exponent n is found to be equal to 0.52 ± 0.02. This low value of n suggests that KSn_2F_5 is a two-dimensional conductor [16].

The temperature dependence of the hopping frequency f_H is shown in figure 3. The value of the activation energy, $E_m = 0.54$ eV, for the migration of charge carriers was obtained from the straight-line fit of the hopping frequency data in figure 3. The E_m value is almost equal to the activation energy of the dc conductivity, $E_\sigma = 0.53$ eV, calculated from the dc conductivity data in figure 3. This implies that the concentration of the mobile charge carriers is independent of temperature and the conductivity is determined primarily by the charge carrier mobility [18].

Recently, renewed interest has been developed regarding the scaling of the conductivity spectra in ion-conducting glasses [19–24]. Usually, the frequency- and temperature-dependent conductivity spectra obey the time–temperature superposition principle (TTSP). This means that, for a given material, the conductivity isotherms can be collapsed to a master curve upon appropriate scaling of the conductivity and frequency axes. The validity of the TTSP can be expressed by the following scaling law of the ac conductivity:

$$\frac{\sigma'(f)}{\sigma_{dc}} = F\left(\frac{f}{f_p}\right). \tag{7}$$

Here, f_p is a characteristic frequency. The master curves of different solids have very similar shapes. However, different scaling approaches have been proposed in order to scale the conductivity spectra not only in terms of temperatures but also in terms of compositions for several glasses. While the value of the dc conductivity σ_{dc} is used as the scaling parameter of the conductivity axis, different forms of the frequency scaling parameter are suggested [19–22]. Some authors have used the hopping frequency of the mobile ions as the scaling

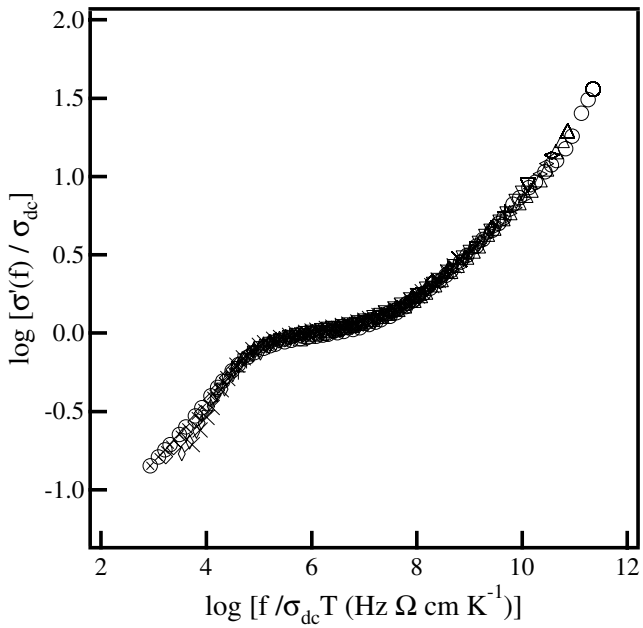

Figure 4. Scaling of the conductivity spectra according to equation (8) for KSn_2F_5.

parameter of the frequency axis [21, 23]. However, Roling *et al* [19, 24] suggested that using $\sigma_{\rm dc}T$ as the scaling parameter of the frequency axis could successfully collapse the conductivity spectra at different temperatures into a single master curve. The scaling law then takes the form

$$\frac{\sigma'(f)}{\sigma_{\rm dc}} = F\left(\frac{f}{\sigma_{\rm dc}T}\right). \tag{8}$$

The main advantage of this scaling law is that it utilizes directly available quantities as scaling parameters of the frequency axis, instead of the arbitrarily determined parameter $f_{\rm H}$.

We present in figure 4 the scaling of the conductivity spectra of KSn_2F_5 in accordance with equation (8), where the values of the dc conductivity $\sigma_{\rm dc}$ were obtained from the fitting of the conductivity spectra according to equation (6). It is clear from figure 4 that the conductivity spectra at different temperatures are successfully collapsed into a single master curve. The scaling of the conductivity spectra using equation (8) indicates that the relaxation mechanism is independent of temperature under the conductivity formalism.

However, considerably more prominent in the literature is the electric modulus formalism, $M^*(f) = 1/\varepsilon^*(f)$. The frequency dependence of $M^*(f)$ for ion conducting materials can be related to a corresponding time-dependent evolution of the electric field resulting from ion motions. However, several researchers have noted discrepancies between interpretations drawn from the analysis of the conductivity and electric modulus formalisms [25–27], and a controversy about which of the two representations provides better insight into the relaxation process in ionic materials is still in debate.

In general, the shape parameter, $\beta_{\rm M}$, determined from the breadth of the electric modulus spectra is found to be larger than that of the conductivity spectra, $\beta_n = 1 - n$ [28], with $0 < \beta_{{\rm M},n} \leqslant 1$. The limit $\beta_{{\rm M},n} = 1$ represents a Debye response. For many glassy ion conductors, the value of $\beta_n = 1/3$ was commonly obtained, while the average value of $\beta_{\rm M}$ was found to be equal to 0.58 [28]. Moreover, recent examinations of the scaling properties

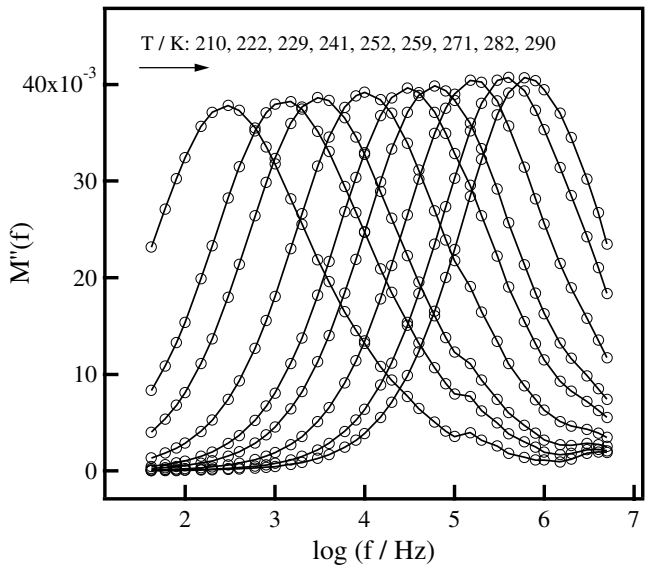

Figure 5. Electric modulus spectra at several temperatures for KSn_2F_5.

of $\sigma^*(f)$ and $M^*(f)$ have shown disturbing differences [19, 24, 29]. For a given material, however, both $\sigma^*(f)$ and $M^*(f)$ exhibit linear scaling as a function of varying temperature, which means that $\sigma^*(f)$ or $M^*(f)$ spectra measured at various temperatures can be scaled so as to collapse to a single master curve.

We introduce in figure 5 the electric modulus spectra, $M''(f)$, for KSn_2F_5 at several temperatures. Well defined asymmetric peaks are observed and the peak position shifts to higher frequency with increasing temperature. The so-called the most probable conductivity relaxation time τ_M could be determined from the relation $2\pi f_{max}\tau_M = 1$, where f_{max} is the frequency at the peak of $M''(f)$. τ_M is found to be thermally activated with activation energy of $E_M = 0.50$ eV, in good agreement with the activation energy value of 0.53 eV determined from the dc conductivity.

The master curve of the electric modulus spectra is shown in figure 6, wherein the frequency axis is scaled by f_{max} and $M''(f)$ is scaled by M''_{max}. It is obvious from figure 6 that the modulus spectra are collapsed to a single master curve, indicating a temperature-independent relaxation mechanism. Moreover, the shape parameter β_M is found to be independent of temperature with a value of 0.52 ± 0.01. This value of β_M is close to that determined from the exponent of the conductivity spectra, $\beta_n = 0.48$. However, we believe that this result is somewhat fortuitous and is limited to low-dimensional conductors (as we have shown above, this value of β_n is influenced by the low-dimensional property of KSn_2F_5 material, whereas β_M is independent of the dimensionality of the conduction space).

Recently, Sidebottom *et al* [30] have studied the influence of the high-frequency dielectric permittivity $\varepsilon'(\infty)$, which is a quantity not related to ion hopping, on the shape of $M''(f)$ spectra, and they found that it is the effect of $\varepsilon'(\infty)$ that produces the characteristic peaked shape of $M''(f)$ spectra. Accordingly, we show in figure 7 the frequency dependence of the imaginary part of the corrected electric modulus, $M^*_C(f) = 1/[\varepsilon^*(f) - \varepsilon'(\infty)]$, after subtracting $\varepsilon'(\infty)$ from the dielectric permittivity data. The value of $\varepsilon'(\infty) = 40$ is used for KSn_2F_5 material. It is clear from figure 7 that the spectra of $M''_C(f)$ have no peaks, in contrast to $M''(f)$, indicating that it may be the influence of $\varepsilon'(\infty)$ that produces the difference in the values of the shape parameters β_M and β_n.

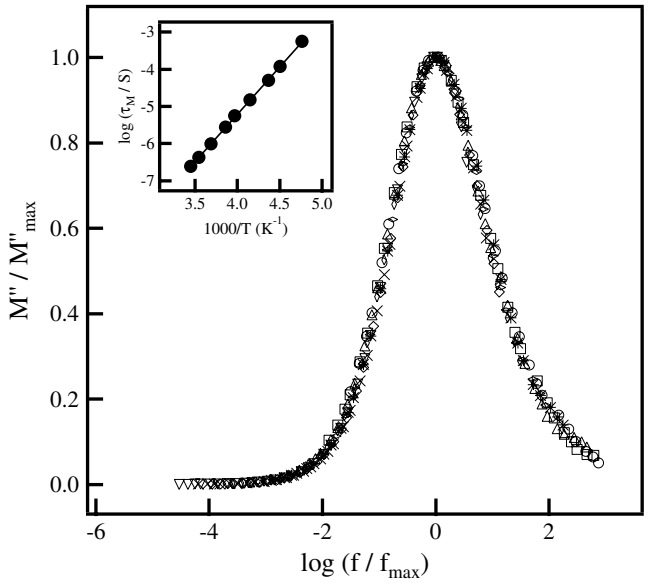

Figure 6. Master curve of the electric modulus spectra. The inset is the temperature dependence of the conductivity relaxation time τ_{M}.

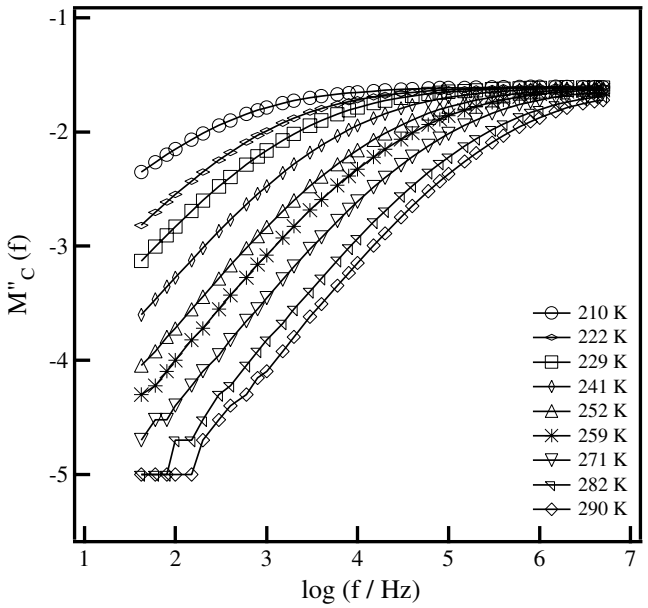

Figure 7. Corrected electric modulus spectra at several temperatures for KSn_2F_5.

According to the coupling model of Ngai [12, 13], the activation energy due to the microscopic movement, or the primitive energy barrier E_{p} for ion jump, is given by the relation

$$E_{\mathrm{p}} = \beta E_{\mathrm{dc}}, \tag{9}$$

where β represents the shape parameter of the conductivity or the electric modulus spectra and E_{dc} is the corresponding activation energy. However, the difference between β_n and β_{M}

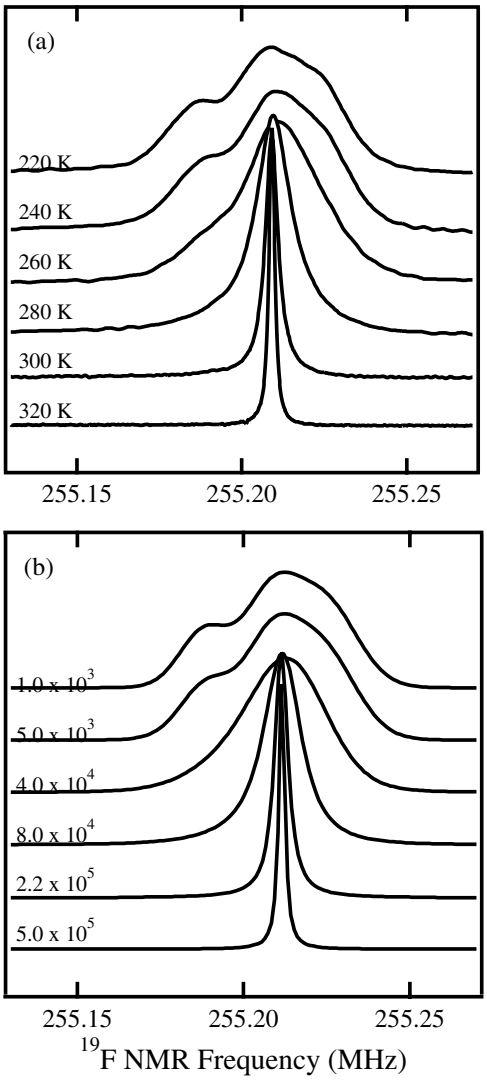

Figure 8. (a) Temperature dependence of the ^{19}F NMR spectra for KSn_2F_5 at several temperatures; (b) simulated spectra with the values of the exchange rate k.

calls into question which method provides the correct insight into the underlying physics of the ion conduction process. In order to answer this question it is useful to consider the activation energy determined from NMR measurements. The activation energy determined from NMR experiments is often observed to be lower than that of the conductivity and corresponds to the local motion [31, 32]. Usually, this activation energy is referred to as the microscopic or primitive energy barrier for ion jump.

Figure 8 shows the ^{19}F NMR spectra in the temperature range from 220 to 320 K, in which the spectrum shows remarkable temperature dependence. In the traditional solid-state ^{19}F NMR using a static sample, motional correlation times can be estimated from the line-width in the narrowing temperature region. In the case of the present high-field experiment, however, the motional narrowing phenomenon is not straightforward because the spectrum is strongly affected by not only dipole–dipole interactions but also chemical shifts due to the

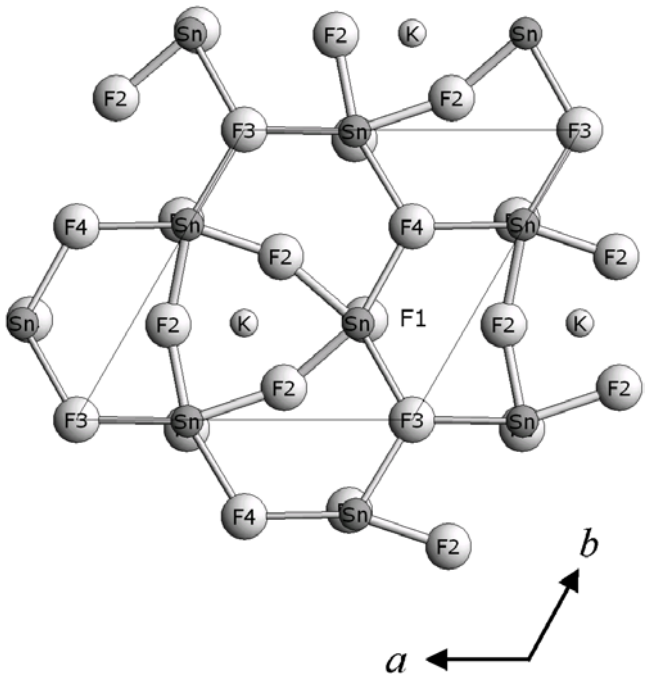

Figure 9. Crystal structure of KSn_2F_5 at 200 K. Only one anionic layer is shown to clarify the bonding scheme.

diffusion of the fluoride ions. In order to get the motional information on the fluoride ions, the spectrum simulation was performed as described below.

Figure 9 shows the structure of KSn_2F_5 projected down to the ab plane at 200 K. The anionic sublattice forms infinite layers in which F(2), F(3) and F(4) sites are not fully occupied [17]. However, four crystallographically different sites were confirmed in the unit cell; these F atoms could be classified into three types based upon the chemical bond. These three fluoride ions are terminal F(1), bridging F(2) and triply bridging F(3) and F(4). As expected from this classification, the rigid lattice spectrum shown in figure 10 could be deconvolved into three Gaussian components which were assigned to the terminal, bridging and triply bridging fluoride ions from the high-frequency side according to the covalent character. The intensity ratio of these components was fixed to 0.40:0.38:0.22 according to the structure at 200 K [17]. With increasing temperature these three components, each of which has a line-width of about 20 kHz, collapse to a single sharp line whose position is given by the weighted average of the three components. In this process, the chemical exchange and the averaging of the dipole–dipole interactions take place simultaneously. In order to estimate the jump rate between a finite set of frequencies, we modified a standard procedure used for chemical exchange phenomena [33, 34]. Under the three-site exchange process, the FID signal $\boldsymbol{G}(t)$ followed by a single rf pulse is given by

$$\boldsymbol{G}(t) = \boldsymbol{A} \cdot \exp(\mathrm{i}\Delta\boldsymbol{\omega}t + \boldsymbol{K}t - \Delta\boldsymbol{H}^2t^2)\mathbf{1} \tag{10}$$

where $\boldsymbol{A}$ is a normalized intensity vector for three sites (A_1, A_2, A_3),

$$\Delta\boldsymbol{\omega} = \begin{pmatrix} \omega_1 - \omega_0 & 0 & 0 \\ 0 & \omega_2 - \omega_0 & 0 \\ 0 & 0 & \omega_3 - \omega_0 \end{pmatrix},$$

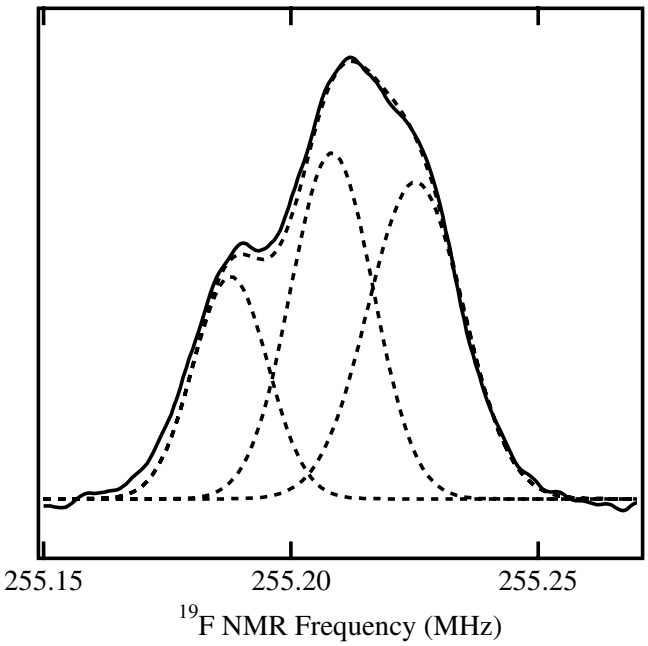

Figure 10. Deconvolution of the ^{19}F NMR spectrum at 180 K for KSn_2F_5. Three components could be assigned to the terminal, bridging and triply bridging fluoride ions from the high-frequency side.

$$\boldsymbol{K} = \begin{pmatrix} -k_{12} - k_{13} & k_{21} & k_{31} \\ k_{12} & -k_{21} - k_{23} & k_{32} \\ k_{13} & k_{23} & -k_{31} - k_{32} \end{pmatrix},$$

$$\Delta\boldsymbol{H} = \begin{pmatrix} 1/T_{21} & 0 & 0 \\ 0 & 1/T_{22} & 0 \\ 0 & 0 & 1/T_{23} \end{pmatrix},$$

and $\mathbf{1}$ is a vector with its all components equal to unity. In these equations, $(\omega_1 - \omega_0)/2\pi$ etc are frequencies from the rf radiation; $\boldsymbol{K}$ is the transition rate matrix defined by exchange rates k_{12} etc. $\Delta\boldsymbol{H}$ is a diagonal matrix with the Gaussian broadening parameters, $1/T_2$, for three components. We assumed $k_{13} = k_{23} = k$ because the number of F sites is proportional to 3:3:2 for terminal, bridge and triply bridging sites, respectively. Furthermore, $k_{12} = k$ was assumed for simplicity. This latter assumption was not so critical because the exchange between F(1) and F(2) sites is performed through F(3) or F(4). Then, the $\boldsymbol{K}$ matrix could be expressed using one rate constant k as

$$\boldsymbol{K} = \begin{pmatrix} -2k & k(A_1/A_2) & k(A_1/A_3) \\ k & -k(1 + A_1/A_2) & k(A_2/A_3) \\ k & k & -k(A_1 + A_2)/A_3 \end{pmatrix}. \tag{11}$$

The simulated spectrum was obtained by the Fourier transformation of $\boldsymbol{G}(t)$ and then compared with the observed one. The exchange rate k and line-width parameter T_2 were estimated simultaneously. Above 240 K a common line-width parameter T_2 was introduced. Figure 8(b) shows the simulations corresponding to the observation temperatures. In the temperature range from 220 to 320 K, the exchange rate is found to be thermally activated with an activation energy value of $E_{\mathrm{NMR}} = 0.29$ eV.

The value of the activation energy E_{NMR} determined from the NMR experiment is clearly smaller than that determined from the electrical relaxation measurements. This value of E_{NMR} may represent the microscopic, or the primitive, energy barrier for an ion jump, as suggested by the coupling model of Ngai [12, 13]. The primitive activation energy E_p determined by equation (9) is equal to 0.25 eV when using the values of β_n and E_σ, while $E_p = 0.26$ eV is obtained using β_M and E_M. These values of E_p agree well with E_{NMR}, in support of the validity of equation (9) in the case of the two-dimensional KSn_2F_5 fluoride ion conductor.

4. Conclusions

We have analysed the conductivity spectra of KSn_2F_5 material using the Almond–West formalism. The relatively small value of the power-law exponent, n, of the conductivity spectra supports the two-dimensional property of the investigated material. The activation energies determined from the temperature dependence of the dc conductivity and the hopping frequency of mobile ions are almost equal, suggesting that the concentration of charge carriers is temperature independent. Moreover, scaling of the conductivity and electric modulus spectra into common curves indicates that the relaxation mechanism is independent of temperature. The activation energy value determined from NMR measurements is mainly due to the local motion of charge carriers, and it is found to be in good agreement with the microscopic activation energy of Ngai's coupling model.

References

[1] Vilminot S and Schulz H 1988 *Acta Crystallogr.* B **44** 233
[2] Vilminot S, Bachmann R and Schulz H 1983 *Solid State Ion.* **9/10** 559
[3] Hirokawa K, Kitahara H, Furukawa Y and Nakamura D 1991 *Ber. Bunsenges. Phys. Chem.* **95** 651
[4] Dyre J C 1988 *J. Appl. Phys.* **64** 2456
[5] Almond D P and West A R 1983 *Nature* **306** 456
[6] Almond D P, Ducan G K and West A R 1983 *Solid State Ion.* **8** 159
[7] Almond D P, Ducan G K and West A R 1985 *J. Non-Cryst. Solids* **74** 285
[8] Jonschor A K 1977 *Nature* **267** 673
[9] Dyre J C 1986 *J. Non-Cryst. Solids* **88** 271
[10] Elliott S R and Owens A P 1989 *Phil. Mag.* B **60** 777
[11] Hunt A 1994 *J. Non-Cryst. Solids* **175** 59
[12] Ngai K L 1979 *Comment. Solid State Phys.* **9** 127
[13] Ngai K L, Rendell R W and Jain H 1984 *Phys. Rev.* B **30** 2133
[14] Funke K 1993 *Prog. Solid State Chem.* **22** 111
[15] Funke K, Roling B and Lange M 1998 *Solid State Ion.* **105** 195
[16] Sidebottom D L 1999 *Phys. Rev. Lett.* **83** 983
[17] Yamada K, Ahmad M M, Ohki H, Okuda T, Ehrenberg H and Fuess H 2003 *Solid State Ion.* submitted
[18] Hairetdinov E F, Uvarov N F, Patel H K and Martin S W 1994 *Phys. Rev.* B **50** 13259
[19] Roling B, Happe A, Funke K and Ingram M D 1997 *Phys. Rev. Lett.* **78** 2160
[20] Sidebottom D L 1999 *Phys. Rev. Lett.* **82** 3653
[21] Ghosh A and Pan A 2000 *Phys. Rev. Lett.* **84** 2188
[22] Schroder T B and Dyre J C 2000 *Phys. Rev. Lett.* **84** 310
[23] Pan A and Ghosh A 1999 *Phys. Rev.* B **59** 899
[24] Roling B 1998 *Solid State Ion.* **105** 185
[25] Almond D P and West A R 1986 *J. Non-Cryst. Solids* **88** 222
[26] Dyre J C 1991 *J. Non-Cryst. Solids* **153** 219
[27] Elliott S R 1994 *J. Non-Cryst. Solids* **170** 97
[28] Sidebottom D L, Green P F and Brow R K 1995 *J. Non-Cryst. Solids* **183** 151
[29] Sidebottom D L, Green P F and Brow R K 1997 *Phys. Rev.* B **56** 170
[30] Sidebottom D L, Roling B and Funke K 2001 *Phys. Rev.* B **63** 024301
[31] Brinkmann D 1992 *Prog. Nucl. Magn. Reson. Spectrosc.* **24** 527
[32] Pradel A and Ribes M 1992 *J. Non-Cryst. Solids* **131–133** 1063
[33] Schmidt-Rohr K and Spiess H W 1994 *Multidimensional Solid-State NMR and Polymers* (London: Academic)
[34] Abragam A 1961 *Principles of Nuclear Magnetism* (London: Oxford University Press) ch 10